Impact of Axial Gradients on Combustion Chamber Acoustics

R. Kaess[1], S. Koeglmeier[2], R. Behr[1], B. Kniesner[1] and T. Sattelmayer[2]

[1]Astrium Space Transportation, Propulsion & Equipment, D-81663 Munich
[2]Lehrstuhl für Thermodynamik, Technische Universität München, D-85747 Garching

Abstract

Combustion instability is a major concern in liquid rocket engine combustion processes. It is based on an interaction between combustion chamber acoustics and combustion process.
The eigenmodes of a full scale combustion chamber with a long cylindrical section are examined in the present study. In experimental data, an axial dependency of the frequency of the dominant T1 eigenmode is seen. There is a lower frequency first tangential eigenmode (T1) which develops close to the face plate and a higher frequency T1 which develops in the downstream area. The development of two different tangential eigenmodes may be caused by different hot gas properties along the axis of the combustion chamber permitting different tangential eigenmodes to form on different axial locations. This phenomenon is assessed numerically using an acoustic tool in the present work.

1 Introduction

Combustion instability has been a topic in the development of liquid rocket combustion engines since the early days of the development of such devices. The phenomenon arises from an interaction between the combustion process in the combustion chamber and the acoustics of the combustion system. Due to this interaction, self-induced pressure oscillations arise. These can reach levels at which they constitute a danger for the safe operation of the engine [1].

1.1 Types of combustion instabilities

Depending, which part of the combustion system is involved, different types of combustion instabilities can be distinguished: Low Frequency combustion instabilities (LF) involve oscillations of the propellant feed system of the engine and typically occur at frequencies of some hundred hertz. In contrast, High Frequency combustion instabilities (HF) involve the acoustics of the combustion chamber and typically result in frequencies in several thousand hertz [3]. Especially, in HF instabilities, large pressure oscillations in the combustion chamber can occur. These oscillations may cause breakdown of the thermal boundary layer and in consequence melting of the combustion chamber wall [1].
Often, combustion instabilities and, especially, HF, have delayed programs and have caused a substantial amount of additional cost. The F-1 engine probably constitutes the most famous example for an engine suffering from HF instabilities [2]. As a consequence, the prediction of such combustion instabilities and, in particular, HF instabilities, has moved into focus of research and various models for the description of this phenomenon exist. In the present time, research on this topic is continued with high effort as the German-French research cooperation REST demonstrates [4].

1.2 Modeling of combustion instabilities

However, still in the present times, the prediction of combustion instabilities remains very challenging. This is due to the fact that a multitude of processes is involved in the occurrence of this phenomenon and the description of all the relevant parts exceeds the presently practicable capacities.
Historically, HF instabilities have been described using frequency domain low order models which consider the combustion chamber mainly as cylindrical volume with rigid walls both on the curved and on the top and bottom boundaries.
Mostly, this cylinder is considered to be filled with a uniform gas corresponding to the hot gas inside the combustion chamber. This model is then combined with a flame response model in order to close the loop between acoustics and combustion process.
The n-τ-model established by Crocco is a famous example for such a flame response model [5].

In the present times, CFD models have gained increasing attention because they offer the possibility of modeling a large amount of processes within one calculation. Also, the usage of CFD for the modeling of the flame and the extraction of the flame response to acoustics is being used. The flame response function is then often combined with acoustic solvers [6].
In the present work, an experimental observation is described and assessed numerically. This observation affects the assumption that the chamber is filled with homogeneous hot combustion products which is often made in low order modeling.

2 Low Order Modeling of HF Instabilities

As HF instabilities have a long history in the development of liquid propellant rocket engines, their modeling has a similarly long history. Low order modeling is still wide spread and is very helpful in assessing the principles of such instabilities.
Real rocket combustion chambers in most cases consist of a cylindrical part of a certain length followed by the convergent part of the nozzle which terminates at the throat and is follow by a divergent part. The parts downstream of the nozzle are not of interest for HF modeling, because the flow is at supersonic speed, there and, hence, acoustic feedback cannot be established with these parts. Commonly, the combustion chamber is modeled as a cylindrical volume corresponding to the cylindrical part of the combustion chamber. Sometimes, this part is elongated by ½ or ⅓ of the length of the convergent part of the nozzle in order to account for this part. In other cases, the nozzle is represented by an acoustic admittance. [7]

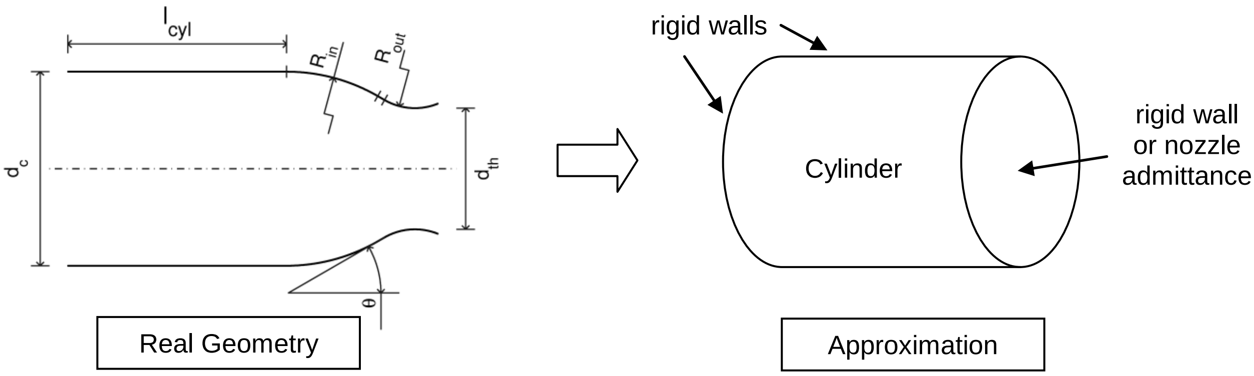

Figure 1: Simplifications commonly applied in low order modeling of combustion stability of rocket combustion chambers

This kind of modeling results as basic solution (all rigid walls, no combustion influence) in the standard eigenmodes of a cylindrical device. These can be well described analytically. The pressure field is given by the formula:

$$p'(r,z,t) = e^{i\omega t}\cos(m\phi)J_m\left(\kappa_{m,n}\frac{2r}{d_c}\right)\cos\left(k\pi\frac{z}{l_{cyl}}\right)$$

This formula is written in terms of longitudinal, tangential and radial Modes with k,m,n being the order of the respective mode. J_m is the m[th] Bessel function and $\kappa_{m,n}$ is the n[th] zero of the first derivative of the aforementioned m[th] Bessel function.
Some values of $\kappa_{m,n}$ for different n and m are given in the following table:

Radial (n)→ ↓ Tangential (m)	0	1	2	3
0	0	3.832	7.016	11.17
1	1.841	5.331	8.536	11.71
2	3.054	6.706	9.970	13.17
3	4.201	8.105	11.35	14.59

Table 1: Values for $\kappa_{m,n}$ for different kinds of eigenmodes

The corresponding eigenfrequency is then given by

$$\omega = a\sqrt{\left(\pi \frac{k}{l_{cyl}}\right)^2 + \left(\frac{\kappa_{m,n}}{d_c/2}\right)^2} \ ,$$

with *a* being the speed of sound of the homogeneous gas in the cylinder
From these formulas, one can see that there is always one defined eigenmode with one corresponding frequency for each combination k,m,n.
Typical eigenmodes obtained in this way are visualized in Figure 2.

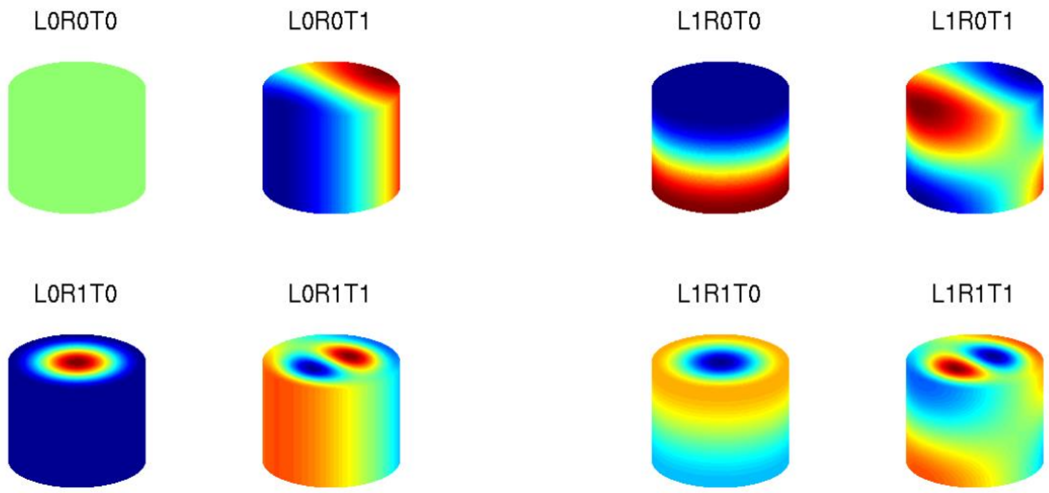

Figure 2: Mode shapes for a cylindrical domain for different Longitudinal, Radial **and** Transversal **(k,n,m) Mode orders. The trivial L0,R0,T0 mode is shown for consistency**

Of course, more sophisticated low order models are available. But, to a large degree, also these models rely on the assumption of homogeneous gas in the combustion chamber [1]. High order models, in turn, are basically capable of capturing nearly all thinkable influences like gradients in the flow, droplets, combustion influence and flow effects.

3 Experimental observations

In the following, measurement data of a full scale engine is presented. As for most of the engines, also for this engine the acoustic eigenfrequencies of the combustion chamber are visible in the spectra for high frequency sampled pressure transducers. This does not imply any instability of the engine, because the chamber acoustics, even when strongly damped, just as any other dynamic system, respond in their eigenfrequencies when being excited by broad band noise (i.e. combustion noise, here).
The combustion chamber features a relatively long cylindrical section. For pure chamber testing a battleship chamber was used being equipped with a total of 6 high speed pressure transducers, 3 of them distributed on the circumference close to the faceplate and the other 3 distributed axially in line with one of the aforementioned ones. Figure 4 illustrates this. No acoustic cavities, baffles or other devices are implemented. Therefore, the chamber wall can be considered as hard walls with a good degree of precision.

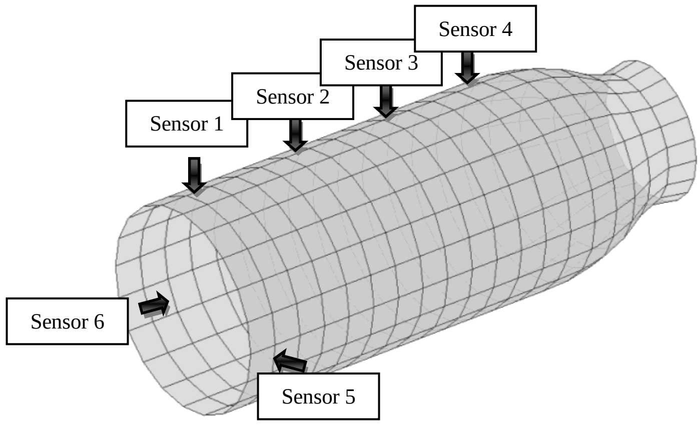

Figure 3: Sketch of the location of the 6 dynamic pressure transducers on the combustion chamber

Now, when the spectra of the sensors are plotted in one diagram, the following can be observed:

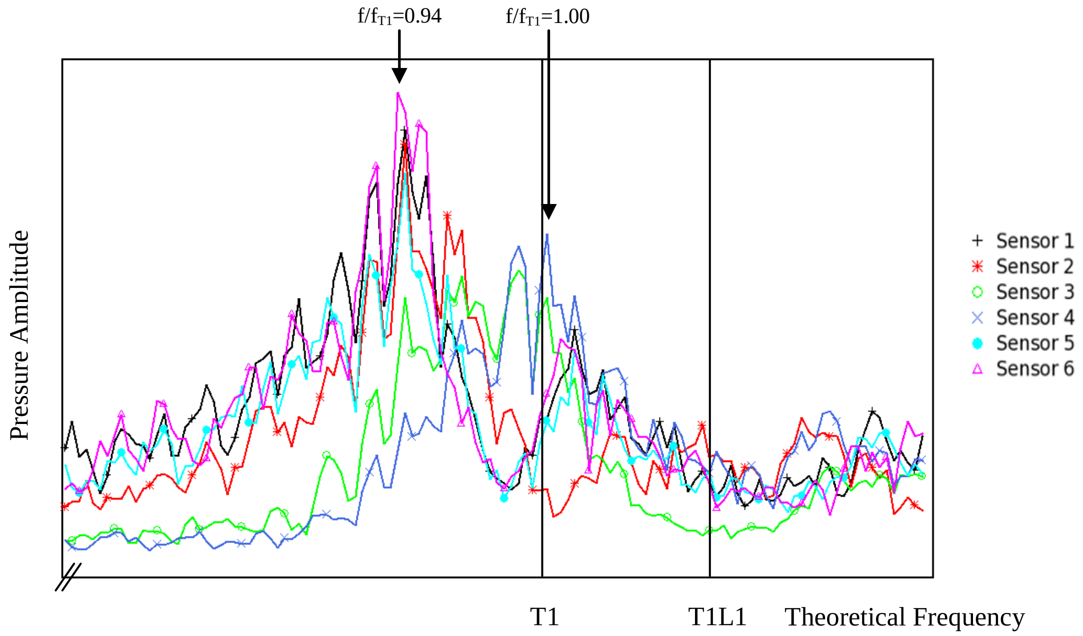

Figure 4: Section around the T1 frequency of the spectrum of the 6 dynamic pressure transducers located in the combustion chamber. T1 and T1L1 denote theoretical eigenfrequencies.

Sensors 1,2,5 and 6 exhibit nearly identical spectra in their dynamic pressure. The peak is located below the theoretical frequency. Sensors 3 and 4, in contrast, differ. These two sensors do not show the peak at the frequency below T1, where the aforementioned four sensors exhibit their peak. They show, in contrast, a peak at a approximately 6% higher frequency, very close to the theoretical T1 frequency.
However, this behavior cannot be explained solely by T1 and T1L1 mode occurrence: A T1 Mode is expected to be present uniformly over a large portion of the cylindrical part of the combustion chamber, whereas a T1L1 mode is expected to have large amplitudes close to face-plate and nozzle with a minimum in-between (see Figure 2). The present data, in contrast show a mode present at the face-plate and a second mode present in the downstream section. These two cannot be explained solely by being T1 and T1L1.

Possibly, this behavior can be explained by the long cylindrical section of the combustion chamber (approx. 2.5 times the diameter) in combination with an axial gradient in the chamber. The axial gradient is generated by the atomization and combustion process and results in a lower sonic velocity in the area of the face plate. The almost fully burnt state, is reached further downstream. In this almost fully burnt region, the sonic velocity corresponds to the sonic velocity assumed for the analytical solution. In either region a T1-mode evolves which can only propagate within the corresponding sonic velocity range. The long cylindrical section provides the downstream mode with sufficient space of uniform diameter to develop. Therefore, it can be observed in this case.

4 Numerical Simulation

In order to validate the hypothesis of the two different T1 Modes present in different parts of the combustion chamber, a numerical simulation has been performed.

4.1 Code

The code employed for the numerical investigation is PIANO-SAT, a derivative of the aeroacoustic solver PIANO originally established by the DLR Braunschweig [8]. PIANO-SAT is currently developed by Astrium and the Technische Universität München, Lehrstuhl für Thermodynamik in order to investigate thermoacoustic instabilities in liquid rocket propulsion systems.
The numerical scheme of PIANO-SAT is based on optimized high order finite differences together with 4^{th} order Runge-Kutta time-stepping which provides a low overall dissipation and dispersion error. The solver admits a variety of different acoustic boundary conditions including wall, neutral, admittance, non-reflective, outflow and radiation. PIANO-SAT solves the Linearized Euler Equations (LEE), Acoustic Perturbation Equations (APE), or Perturbed Nonlinear Nonconservative Euler Equations (PENNE) in the time domain on structured 2D or 3D grids. For the present application, the Linearized Euler Equations have been chosen.

4.2 Computational Mesh

The computational domain consists of a cylindrical combustion chamber followed by a convergent-divergent nozzle section. This geometry is meshed using the commercial tool ICEM. An O-grid topology is employed to devide the computational domain into five blocks. The central block has a resolution of 21x21x156 points whereas each of circumferential blocks consists of 21x15x156 points. Hence, the thrust chamber is resolved by 265356 grid points. The grid is slightly refined towards the face plate using a stretching ratio of 1.01 in combination with a hyperbolic bunching law.

4.3 Boundary Conditions and Acoustic Excitation

At the injector face a chocked inlet boundary condition (dm'/dt = 0) is applied. This type of boundary condition is characterized by a vanishing acoustic energy flux [9] and as a result the combustion chamber is decoupled from the feed system. The convergent-divergent nozzle is operated in chocked condition and provides a natural non-reflective acoustic boundary due to the fact that disturbances cannot propagate upstream once they reached the supersonic flow region. For numerical reasons an additional absorbing sponge layer is placed within the divergent nozzle section to avoid the accumulation of acoustic energy. Combustion chamber walls are considered as fully reflective slip walls.
The simulation is excited with a pressure pulse of Gaussian spatial distribution which provides a broadband excitation for most of acoustic modes. The centre of the pressure pulse is located off axis in the downstream half of the cylindrical combustion chamber section where the mean flow properties are almost homogeneous.

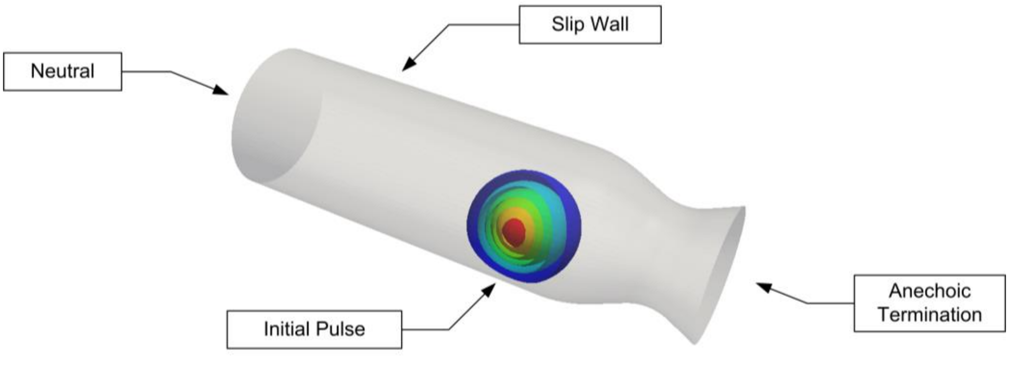

Figure 5: Boundary and initial conditions. A spatially Gaussian pressure pulse provides a broadband excitation for most of the acoustic modes.

4.4 Mean Flow Field

In order to solve the Linearized Euler Equations (LEE) a representative mean flow field is required. For this purpose a multi-step process has been used.
In the first step a 2D axisymmetric RANS-simulation of the reacting flow field within the combustion chamber is performed using Astrium's in-house code Rocflam-II [10]. The results of this steady state simulation are averaged in the radial direction and are superimposed with a non-reacting 3D Euler solution of the mean flow field within the nozzle section using a blending technique. The final composite solution is characterized by gradients with are strictly axial in the cylindrical section and fully three-dimensional in adjacent nozzle section of the combustion chamber.
To improve the conditioning of the solver matrices all flow quantities are non-dimensionalized with appropriate reference values.

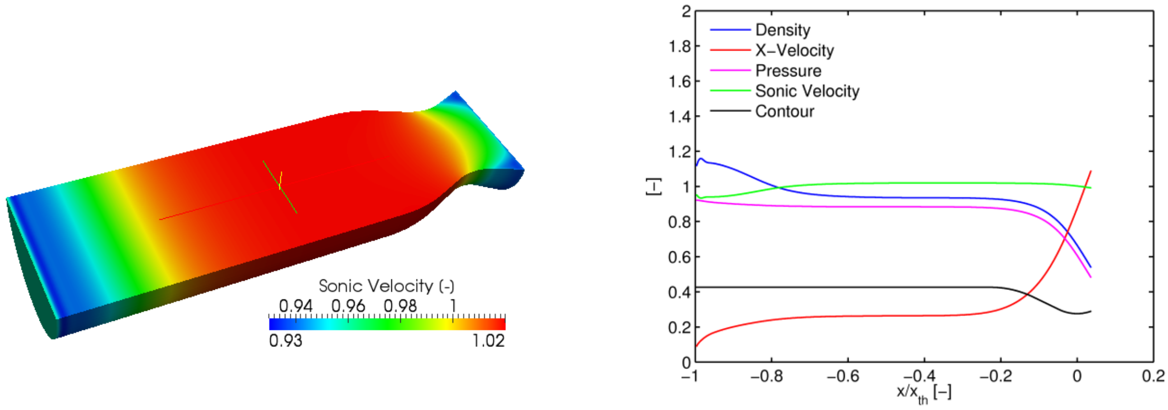

Figure 6: Mean flow field for the sonic velocity (left) and axial variation of the mean flow quantities along the axis of symmetry (right); all quantities non-dimensional.

5 Results

As already mentioned the results of PIANO-SAT are given in the time domain. In order to distinguish between different modes and oscillation frequencies the time domain data is analyzed using the method of dynamic mode decomposition (DMD). Dynamic mode decomposition is an Arnoldi-like method which attempts to extract dynamic information in terms of coherent structures (mode shapes) and corresponding eigenvalues from a sequence of spatially distributed data (snapshots). Regarding details about this algorithm the reader is referred to [11].
For the application of dynamic mode decomposition to the present simulation a series of snapshots is generated by sampling the transient results on the surface walls of the cylindrical combustion chamber section. This drastically reduces the amount of data included within the post-processing step.

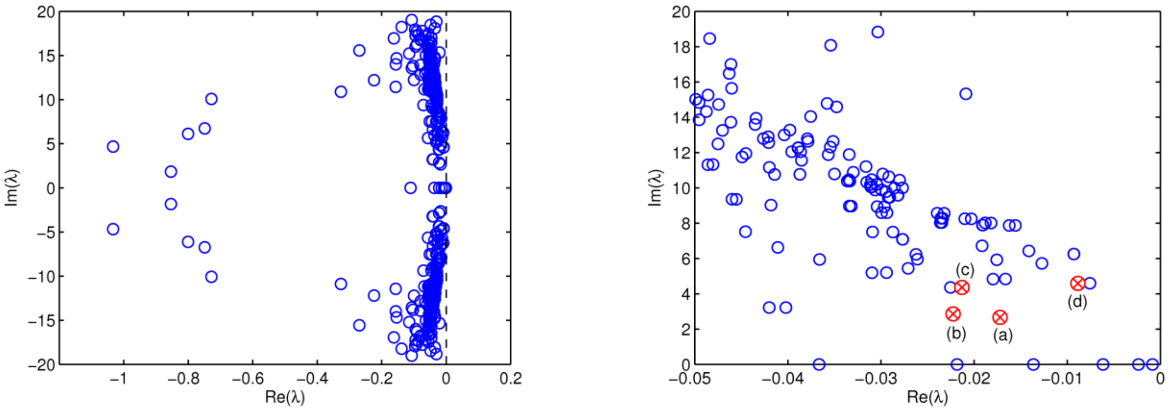

Figure 7: DMD-spectrum of nondimensional eigenvalues; very high damping rates are linked with nonphysical modes.

The DMD-spectrum extracted from the recorded series of snapshots is displayed in Figure 7. The imaginary part of the eigenvalues λ corresponds to the nondimensional frequency of the modes. The real part of λ represents the nondimensional damping rate. All eigenvalues are oriented on the left side of the complex plain which means that the system is overall damped. A strong orientation to the neutral axis is visible where eigenvalues characterized by very high damping rates are linked with nonphysical modes.

In Figure 8 four modes associated with the labeled eigenvalues of Figure 7 are shown. Modes (a) and (b) are clearly identified as first transverse modes (T1). The amplitude maximum of mode (a) is located close to the injector face plate (z = 1) of the combustion chamber whereas the amplitude maximum of mode (b) is located near the entrance plain of the convergent-divergent nozzle (z = 0). With respect to mode (a) the oscillation frequency of mode (b) is shifted to higher values (≈ 8%). This behavior is in line with the experimental observations where a similar shift of the oscillation frequency to higher values is seen. Modes (c) and (d) are characterized as second transverse modes (T2). Aside from that, these modes show an analogous behavior regarding amplitude maximum and frequency shift to modes (a) and (b).

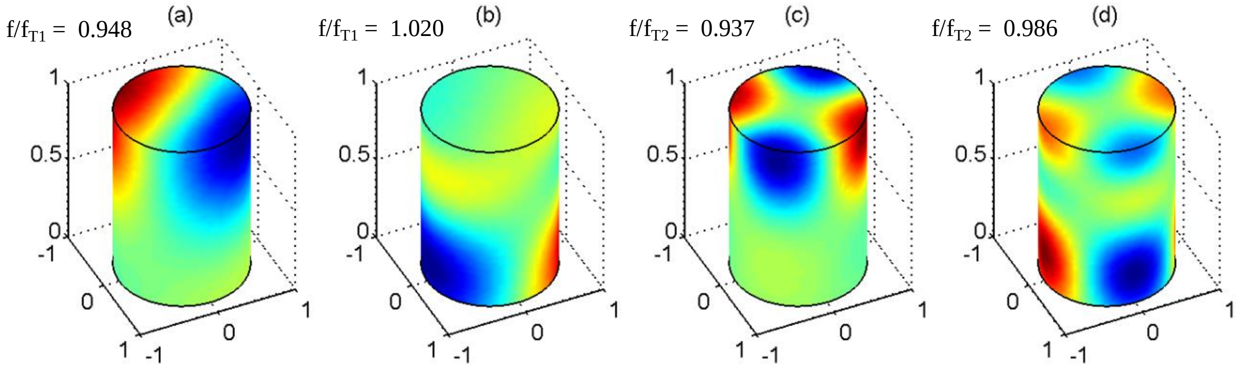

Figure 8: Representative dynamic modes (real part) associated with the spectrum of Figure 7; all dimensions nondimensional. Frequency is nondimensionalized with theoretical eigenfrequency.

It shall be mentioned that the same analysis has also been carried out for an identical configuration but without axial mean flow gradients inside the cylindrical combustion chamber section. In the absence of axial gradients a behavior comparable with the results shown in Figure 8 could not be identified. It can therefore be concluded that axial gradients in combination with a long combustion chamber may indeed be the origin for the observed axial dependency of resonance frequencies within experimental data.

6 Conclusions

An axial dependency for the frequency of the dominant T1 eigenmode has been observed within experimental data. The hypothesis of two different tangential eigenmodes caused by different hot gas properties along the axis of the combustion chamber has been investigated on the basis of a numerical simulation. The results of this simulation have been analyzed using dynamic mode decomposition (DMD). The computed mode shapes and oscillation frequencies suggest that axial mean flow gradients contribute to the development of lower frequency tangential eigenmodes close to the face plate and higher frequency modes in the downstream area.

7 Acknowledgements

The development of the Piano code is supported by the German Space Agency “Deutsches Zentrum für Luft- und Raumfahrt e.V.” (DLR) with funds from the German Federal Ministry of Economics and Technology under grant No. 50RL1040. Financial support is also granted by DLR in the frame of the TARES-Program. The financial support is gratefully acknowledged.

References

[1] Harrje, D. and Reardon, F. (ed.). *Liquid Propellant Rocket Combustion Instability.* NASA SP-194. National Aeronautics and Space Administration, 1972

[2] Oefelein, J. and Yang, V. *Comprehensive Review of Liquid-Propellant Combustion Instabilities in F-1 Engines.* Journal of Propulsion and Power, 1993, 9, 657-675

[3] Preclik, D. & Spagna, P. *Low Frequency and High Frequency Combustion Oscillation Phenomena Inside a Rocket Combustion Chamber Fed by Liquid or Gaseous Propellants* AGARD CP 450, 1988, 1-18

[4] Various authors, Proceedings of the 2nd REST Modelling Workshop, October 5/6 2010, Ottobrunn, 2011

[5] Crocco, L. and Cheng, S. *Theory of Combustion Instability in Liquid Propellant Rocket Motors.* AGARDograph No.8. Butterworths Scientific Publications, 1956

[6] Ramcke, T., Schmid, M. and Sattelmayer, T. *Response Characterization of a LOX-GH2 Flame to Forced Acoustic Pressure Fluctuations*. 5th European Conference for Aeronautics and Space Sciences, München, Germany. 2013.

[7] Mitchell, C. *Analytical Models for Combustion Instability*. In Yang, V.; Anderson, W. & Zarchan, P. (ed.). *Liquid Rocket Engine Combustion Instability*. American Institute of Aeronautics and Astronautics, Inc., 1995

[8] Delfs, J., Bauer, M., Ewert, R., Grogger, H., Lummer, M. and Lauke,T.. *The Prediction of Three-Dimensional Liquid-Propellant Rocket Nozzle Admittances Numerical Simulation of aerodynamic noise with DLR's aeroacoustic code PIANO.* Deutsches Zentrum für Luft- und Raumfahrt e.V. in der Helmholtz-Gemeinschaft, Institut für Aerodynamik und Strömungstechnik, Abteilung Technische Akustik, Braunschweig, Germany, January 2008

[9] Cantrell, R. and Hart, R. *Interaction between Sound and Flow in Acoustic Cavities: Mass, Momentum and Energy Considerations.* The Journal of the Acoustical Society of America, 36(4), 1964

[10] Frey, M., Kniesner, M. and Knab, O. *Consideration of Real Gas Effects and Condensation in a Spray Combustion Rocket-Thrust-Chamber Design Tool*. Progress in Propulsion Physics - Volume 2, pp. 285-296, 2011.

[11] Schmid, P. *Dynamic mode decomposition of numerical and experimental data.* Journal of Fluid Mechanics, 656, pp 5-28, 2010